Ratio of the Effective Charge of He Beams Traversing Gaseous and Metallic Cadmium*

W. MECKBACH†
Centro Atómico Bariloche, San Carlos de Bariloche, Argentina
AND
S. K. ALLISON
The Enrico Fermi Institute for Nuclear Studies, The University of Chicago, Chicago, Illinois
(Received 9 May 1963)

By successively measuring the energy degradation of He and H beams of the same velocity in the same Cd foil and in the same Cd-vapor absorber at $\sim 160\,\mu$ pressure, ratios of the stopping power for He to the stopping power for H at the same velocity (ϵ_{He}/ϵ_H) and accurate to $\sim 1.3\%$ were obtained. These extend from beam velocities of 1.2 to 3.0 in units of $e^2/\hbar$; in He kinetic energies from 148 to 920 keV, and cover the region in which the square of the effective charge of the beam is changing most rapidly due to electron capture and loss. Comparison of these ϵ_{He}/ϵ_H ratios in the attenuated gas and in the metal should indicate whether the effective number of electrons attached to the He nucleus in the gas remain attached to it as it traverses the metal. The changes found are fractionally much smaller than those found by Lassen in fission fragments, and Roll and Steigert in fluorine ions. For He ions between 575- and 920-keV energy, the effective charge in the gas seems higher than in the solid, constituting a reversal of the anticipated effect. Empirically, a knowledge of ϵ_{He}/ϵ_H ratios is useful for the conversion of data on absolute stopping powers for H into He and vice versa. In the kinetic energy range above 1 MeV per amu, Roll and Steigert and Lassen have found that such ratios for fluorine ions, for instance, fall into two groups characteristic of solids as a class and gases as a class. Comparison of the results reported here with ϵ_{He}/ϵ_H ratios obtained by combining results of various experimenters indicates that such a division is not indicated for ϵ_{He}/ϵ_H at lower energies per amu, but that the difference between solids and gases is comparable to the differences between different metals and different gases.

I. INTRODUCTION

FOR a beam composed of particles of mass M and atomic number Z travelling at velocity V, there is a high-energy region, corresponding to

$$V \gg Ze^2/\hbar, \tag{1}$$

in which the projectiles remain entirely stripped of their extranuclear electrons. For translational velocities comparable to the above limit, the charge of a projectile can no longer be considered constant since electrons become attached to it and are temporarily or permanently retained.

If the beam is not divergent and is traveling in charge equilibrium in a uniform target medium, let us designate the fractions of the projectiles in the various possible charge states by appropriate values of $F_{i\infty}$, where i is a positive or negative integer or zero corresponding to the charge in units of the magnitude of the electronic charge.

The Average Charge of a Particle Beam

The average charge of such a projectile beam may be considered in the following different ways:

If the beam is collected in a Faraday cup and the net accumulation of charge in electron units, from a known number of entering projectiles is measured, the quotient $\bar{i}$ is a measure of the average charge.

If the beam passes into high vacuum, and its charged components are separated and measured in a magnetic field, the fractions $F_{i\infty}$ become known, and it is clear that

$$\bar{i}=\sum iF_{i\infty}. \tag{2}$$

Another charge average may be obtained if the stopping power for the beam is measured, and from it an average of the squares of the component charges obtained. The atomic-stopping power or specific-energy loss of the beam per target atom is

$$\epsilon=-(1/N)dE/dx, \tag{3}$$

where N is the number of target atoms per cm^3 and dE/dx the rate of change of projectile energy per centimeter of path. The concept of average charge as determined by stopping power seems useful mainly for heavy ions in the energy range 1–10 MeV per amu, where two or more electrons have been removed from every projectile. It is customary for workers in this field to discuss $\mathcal{E}_M$, the energy per amu, that is, per unit of physical atomic weight. Thus $E=M\mathcal{E}_M$. Furthermore, it is convenient to change the scale of length in Eq. (3), replacing dx as follows:

$$dx=(M/Z^2)dx_M \tag{4}$$

and, thus,

$$\epsilon_{M,Z}=-(1/N)d\mathcal{E}_M/dx_M=Z^{-2}\epsilon. \tag{5}$$

In order to avoid confusion with i and $\bar{i}$, we will, in deducing an average charge from stopping power, use z instead of i to represent the charge of a beam component. If the velocities for a certain beam are in the

* This work was supported in part by the U. S. Atomic Energy Commission.
† Fellow of the Argentine National Research Council.

high-energy region previously specified, so that the projectiles are all bare nuclei of charge Z, the Bethe-Bloch equations[1] for an unscreened nucleus as a projectile give

$$\lim_{v>>1} \epsilon = Z^2 f(v) \tag{6}$$

or

$$\lim_{v>>1} \epsilon_{M,Z} = f(v), \tag{7}$$

where v is the velocity in units of $e^2/\hbar$, or $v=\hbar V/e^2$. Guided by this prediction we may formally express the $\epsilon_{M,Z}$ of a beam in the capture and loss region as

$$\epsilon_{M,Z} = (\langle z^2\rangle_{\rm av}/Z^2) f(v) = \gamma^2 f(v), \tag{8}$$

with

$$\lim_{v>>1} \gamma^2 = 1. \tag{9}$$

In the energy range above 1 MeV per amu, a hydrogen beam consists entirely of protons, so that $Z=\langle z^2\rangle_{\rm av}=1$; thus, the γ^2 of a heavy-ion beam may be determined by

$$\gamma^2 = \epsilon_{M,Z}/\epsilon_{M,1}, \tag{10}$$

in which $\epsilon_{M,1}$ is the modified stopping power [Eq. (5)] for hydrogen.

We now discuss the question as to whether there is any simple relation between γ^2, or $\langle z^2\rangle_{\rm av}$, and the $F_{i\infty}$ values of the charge components of the beam as revealed by magnetic analysis.

A simple relationship is predicted by an interpretation of the stopping of a partially stripped beam advanced by Knipp and Teller.[2] It is assumed that the total specific energy loss of the beam can be expressed as the weighted sum of energy losses appropriate to each of its charge components, and, furthermore, that each such partial stopping power can be expressed as in Eq. (6). Thus,

$$\epsilon = f(v)\sum i^2 F_{i\infty}, \quad \text{or} \quad \epsilon_{M,Z} = f(v) Z^{-2} \sum i^2 F_{i\infty}, \tag{11}$$

and from Eq. (10)

$$\gamma^2 = \langle i^2\rangle_{\rm av}/Z^2, \quad \text{where} \quad \langle i^2\rangle_{\rm av} = \sum i^2 F_{i\infty}. \tag{12}$$

Objections to such a simple interpretation as that underlying Eq. (11) may readily be advanced. Energy losses in the capture and loss cycle have not been allowed for, neither has a type of loss in which the electrons adhering to the projectile are excited but not ionized.

Nevertheless, Eq. (12) has been verified by Northcliffe[3] for an oxygen beam emerging from an aluminum foil. The values of $F_{i\infty}$ were obtained by magnetic analysis, using intensity estimates of images on a photographic plate. In the lower kinetic energy ranges with $\mathcal{E}_M$ from 1 to 3 MeV per amu, values of i from 5 to 8 inclusive were detected; in the higher energy range from 6 to 10 MeV per amu only $i=7$ and $i=8$ were observed. The modified stopping powers $\epsilon_{M,Z}$ were observed for energy losses in aluminum and γ^2, obtained by taking the ratio of these to the modified stopping power for hydrogen at the same velocity (that is, the same $\mathcal{E}_M$) computed from an empirical formula due to Bichsel.[4] Equation (12) was established to within 2% between 2.5 and 9 MeV per nucleon.

In spite of this success for the highly stripped oxygen ions, the statement of Eq. (12) is almost certainly not correct for low values of i and low energies. Allison *et al.*[5] and Huberman,[6] for instance, have shown that in a 60-keV hydrogen beam in hydrogen gas, where $F_{0\infty}=0.45$ and $F_{1\infty}=0.55$, about 32% of the energy losses are due to collisions in which the charge of the projectile is changed, and 16% in energy losses caused by H^0 collisions in which the atomic projectiles remain neutral after the impact. Neither of these energy losses appear in the sum of Eq. (11).

II. STATEMENT OF THE PROBLEM AND DISCUSSIONS OF PREVIOUS WORK

A. A Density Effect on the Effective Charge

It is obvious that in a gas the fractions $F_{i\infty}$ will depend on the velocity of the projectiles, on their atomic number, and on the "chemical" nature of the target material. For instance, to illustrate the effect of the target material, the fraction $F_{1\infty}$ of a hydrogen beam in protonic form is different, at the same velocity, in the gases H_2 and O_2, and probably has a third and different value in H_2O gas.

Evidence of a density effect on the $F_{i\infty}$ fractions was first obtained by Lassen[7–9] in his experiments on the charges of fission fragments traversing various gases.

The effective charge of the light fragment, defined as in Eq. (2) and determined by magnetic analysis, increased in argon as the pressure increased, rising from 15.3 at 1–2 mm Hg to 17.2 at 20 mm, followed by a very slow increase to 17.7 at 140 mm. But the total variation from gas to gas, and with pressure in a given gas, was small compared to a large difference which appeared between gases and solids. For instance, heavy fragments of velocity about $v=3$ or 6.6×10^8 cm/sec had $\bar{i}$ ranging from 9.2 to 10.4 in various gases, but on emerging from mica had $\bar{i}=18.0$.

---

[1] H. A. Bethe and J. Ashkin, in *Experimental Nuclear Physics*, edited by E. Segré (John Wiley & Sons, Inc., New York, 1953), Vol. I, Part II.
[2] J. Knipp and E. Teller, Phys. Rev. **59**, 659 (1941).
[3] L. C. Northcliffe, Phys. Rev. **120**, 1744 (1960).
[4] H. Bichsel, Phys. Rev. **112**, 1089 (1958).
[5] S. K. Allison, J. Cuevas, and M. Garcia-Munoz, Phys. Rev. **127**, 792 (1962).
[6] M. N. Huberman, Phys. Rev. **127**, 799 (1962).
[7] N. O. Lassen, Kgl. Danske Videnskab. Selskab, Mat. Fys. Medd. **26**, No. 5 (1951).
[8] N. O. Lassen, *On the Total Charges and the Ionizing Power of Fission Fragments* (E. Munksgaards Forlag, Copenhagen 1952).
[9] N. O. Lassen, Kgl. Danske Videnskab. Selskab, Mat. Fys. Medd. **30**, No. 8 (1955).

Bohr and Lindhard[10] have interpreted both the pressure effect in gases and the large gas-solid difference as a density effect. They assume that in a high density medium many of the beam ions will remain in excited states between collisions, thus favoring electron detachment in subsequent encounters and shifting the effective charge toward higher positive values.

Our experiments were undertaken to provide information pertinent to the following question: Does the charge composition of a helium beam depend on the phase (solid or gas) of the material being traversed? Two phases will, in general, differ in density, and certainly also the rarefied, gaseous phase and the condensed, solid phase of the same element will differ in the quantum energies of their electrons. Both differences might affect the equilibrium charge density of the beam.

B. Previous Evidence in H and He Beams

For H and He beams there is no conclusive evidence for a large difference in effective charge between gaseous and solid ambient materials. In 1953 Allison and Warshaw[11] compared the then existing data on the ratio He^{++}/He^{+} for a helium beam in charge equilibrium in air, and in a helium beam which had been scattered at 85°16′ from gold into high vacuum. The scattered beam showed a He^{++}/He^{+} ratio higher by almost a factor of 2, which was taken as indicating that in traversing the metal, as compared to the gas, the beam contains a higher fraction of He^{++}. This conclusion, seen in retrospect, was probably not justified; the most serious objection against it being that it selected particles which had been scattered through a large angle and, thus, through collisions in which the electronic structure of target and projectile were deeply penetrated.

As Everhart[12] and his associates have shown, such large-angle scatterings greatly increase the effective charge of the scattered projectiles. For instance, a 100-keV helium beam in rectilinear motion through argon gas has $F_{2\infty}=0.0026$,[13] but the He projectiles scattered at 16° from argon have $F_2=0.04$. Thus, the angular deviation produces a high value of F_2, which may not be reduced to the $F_{2\infty}$ characteristic of an unidirectional beam making electronic encounters in the metal before the projectiles emerge into high vacuum.

Experimental results are now available concerning the charge composition of H and He beams which have passed through solid foils, thus avoiding the objection of a charge enhancement due to large-angle scattering. Allison[14] has collected data on the charge composition of such beams emerging from solids,[15–17] and compared them with measurements in gases. In the case of hydrogen beams up to 200 keV emerging from fresh Al foils, the $F_{1\infty}$ is intermediate between that observed at the same velocity for hydrogen projectiles in H_2 and N_2 gases.

Thus, any effect characteristic of the solid or gaseous phase of a target material is obscured by the larger "chemical" differences between the three ambient substances in question.

In the case of helium beams below 500 keV in kinetic energy, the He^{++}/He^{+} ratios emerging from metal foils seem higher than in some gases (air and hydrogen) but close to those observed in neon gas.

In the case of heavier projectiles, Nikolaev *et al.* (see Ref. 17) have investigated B, N, O, Ne, and C atomic and ionic beams in various gases and emerging from Celluloid. They find $\bar{i}$ [Eq. (2)] for a 7.0-MeV boron beam to be 4.4 in H_2 gas, 3.9 in air and in argon, and 4.0 in high vacuum after emerging from solid foils. For a 3-MeV beam, the numbers are 3.0 (H_2), 3.2(air), 3.4(Ar), and 4.6(Celluloid), showing some enhancement in the emergent beam from the Celluloid.

The experimental work on H and He beams which has been mentioned, like that reported in the present paper, has been carried out at relatively low-beam velocities, below that corresponding to 1-MeV kinetic energy for He projectiles. In spite of the fact that these beams actually traversed the foils, there remain objections, more likely to be valid at these low energies, to the implicit assumption that the values of F_i in the emergent beam from the solid are equal to the values $F_{i\infty}$ which the beam had in the solid before emerging into high vacuum. Two such objections are the following:

(1) There is a work function on escaping through the solid surface into vacuum, and this may considerably affect the number of electrons attached to the ion as it leaves the solid.

(2) A possible source of experimental error lies in the fact that, in solids, equilibrium is attained in extremely thin layers. Hence, equilibrium fractions obtained by letting a beam traverse a foil may actually only be typical of contaminations on the surface of emergence.

Phillips[16] has studied this second effect quantitatively. He finds, for example, that for a 20-keV hydrogen beam in Al, the measured proton component is more than 40% higher for an "old surface" than for freshly deposited aluminum. Thus, the apparently uniform

[10] N. Bohr and J. Lindhard, Kgl. Danske Videnskab. Selskab, Mat. Fys. Medd. **28**, No. 7 (1954).
[11] S. K. Allison and S. D. Warshaw, Rev. Mod. Phys. **25**, 779 (1953).
[12] E. N. Fuls, P. R. Jones, F. P. Ziemba, and E. Everhart, Phys. Rev. **107**, 704 (1957).
[13] C. F. Barnett and P. M. Stier, Phys. Rev. **109**, 385 (1958).
[14] S. K. Allison, Rev. Mod. Phys. **30**, 1137 (1958); cf. Fig. VI-8, p. 1167.
[15] G. A. Dissanaike, Phil. Mag. **44**, 1051 (1953).
[16] J. A. Phillips, Phys. Rev. **97**, 404 (1955).
[17] S. Nikolaiev, I. S. Dmitriev, L. N. Fateeva, and Ya A. Teplova, Zh. Eksperin. i Teor. Fiz. **33**, 1325 (1957) [translation: Soviet Phys.—JETP **6**, 1019 (1958)]. The data in this paper on the composition of helium beams emerging from mica were not included in Fig. VI-8 of the review by Allison (Ref. 14) but agree well with those observed by others from solids other than gold.

charge composition found by Hall[18] in hydrogen beams and by Dissanaike[15] in helium beams emerging from various metals may have been due to a common surface layer, typical of the vacuum he used rather than the foil material.

However, there is evidence that for highly stripped ions with $\mathcal{E}_M$ above approximately 2 MeV/nucleon, the emergent charge distribution is typical of that in the traversal of the solid. Reynolds *et al.*[19] investigated the charge composition of 26-MeV nitrogen beams emerging from zapon foils. Foils could be prepared which were so thin (4 μg/cm^2) that charge equilibrium in the transmitted beam was not attained until several foils had been inserted. Thus, the approach to the equilibrium values $F_{i\infty}$ could be studied, and demonstrated to be dependent on foil thickness rather than surface conditions. Also Northcliffe's experiments[3] on the equality of γ^2 and $\langle i^2\rangle_{\rm av}/Z^2$ for oxygen beams emergent from aluminum foils, which we have previously discussed, indicate that the emergent charge ratios are typical of conditions inside the metal, since surface conditions can have little effect on the total loss of energy in the foil, from which γ^2 is calculated.

C. Evidence from Beams of High-Energy per Nucleon

Roll and Steigert[20] have published evidence for a density effect in the effective charge of highly stripped heavy ions of energies 1 to 10 MeV/amu [velocity $=(1.4\text{–}4.4)\times10^9$ cm/sec]. As a measure of the effective charge of the beam, γ^2 from Eq. (10) has been used. The value of γ^2 for F^{19} projectiles of 1.9×10^9 cm/sec velocity is 0.65 in oxygen and argon gases, but such a fluorine beam emerging from a nickel or aluminum foil has $\gamma^2=0.76$, a 17% increase. Beams of other light elements near fluorine give similar results. According to Bohr and Lindhard,[10] the maximum change in γ^2 from a very diffuse gas absorber giving ample time for electromagnetic energy release between collisions to a solid, would be 44%.

III. PLAN OF THE EXPERIMENT

As previously stated, our experiments were undertaken to investigate changes in charge composition of a helium beam which might result from entering a solid after having attained charge equilibrium in a rarefied gas. From the Bohr and Lindhard interpretation,[10] such a change would be primarily ascribed to a density effect rather than to a difference in the ambient electronic environment. However, to minimize such "chemical" effects, and simplify the interpretation of changes if found, we decided to use two phases of the same element as stopping material, namely, cadmium metal and cadmium vapor. In order to avoid the possibility of surface effects in the foils, it was decided to measure the effective charge by specific energy loss [i.e., by γ^2 of Eq. (10)] rather than by magnetic analysis of the beam [i.e., by i of Eq. (2)]. It could be estimated that, in an absorption tube 50-cm long, sufficient cadmium vapor for a 10% energy decrement could be produced at 325°C, and that the necessary cadmium foils would be about 50 μg/cm^2, both gas and solid, therefore, being attainable under simple experimental conditions.

Since the experiment was directed at γ^2 of Eq. (10), only ratios of stopping powers needed to be measured, and no absolute values were attempted. This greatly simplified the experiment by avoiding weighing of the foils, and making it only necessary to hold the temperature of the Cd-vapor vessel constant long enough to complete the measurement of the energy decrement of a helium beam and a hydrogen beam of equal velocity. Since, with a mixture of hydrogen or deuterium and helium in the ion source, the accelerator would simultaneously produce the two beams, the comparison could be made in an interval of minutes. It was not necessary to measure the distribution of temperature along the vapor cell, nor the absolute density of Cd atoms/cm^3.

The energy range which could be investigated was limited to the operating range of the accelerator, from 75 to 460 kV. Fortunately, this covered most of the range of greatest interest, i.e., the electron capture and loss region in which the helium beam changes from predominantly He^0 to predominantly He^{++}. Figure 1 shows the ratio of the stopping power of argon gas[21–24] for a

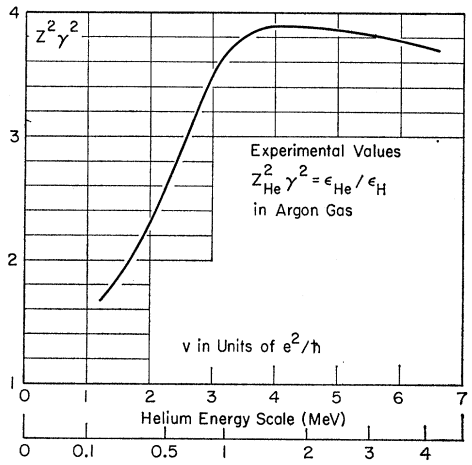

FIG. 1. The ratio of the atomic stopping powers of argon gas for He and H beams of the same velocity. The rising curve from 0.1- to 1.5-MeV He kinetic energy is due to the stripping of electrons from the H and He projectiles.

[18] T. Hall, Phys. Rev. **79**, 504 (1950).

[19] H. L. Reynolds, L. D. Wyly, and A. Zucker, Phys. Rev. **98**, 474 (1955). See also H. H. Heckman, E. L. Hubbard, and W. G. Simon UCRL-10265 (unpublished), who failed to find evidence for surface effects at high energies.

[20] P. G. Roll and F. E. Steigert, Phys. Rev. **120**, 470 (1960).

[21] Data for He in argon by M. Burgy, reported in S. K. Allison and M. Garcia-Munoz, "The Penetration of Matter by Heavy Ions of Kinetic Energies below 1 MeV per Unit Atomic Weight." A report by the Subcommittee on the Penetration of Charged

helium beam to its stopping power for hydrogen at equal velocities from $v=1.2$ to 6.5. At higher velocities there is no indication that the ratio is approaching the expected value of 4; it remains between 3.8 and 3.9, an effect not yet explained. The charge-changing region for helium apparently lies below about $v=4$ or 1.6-MeV helium kinetic energy. Our measurements in Cd vapor and metal extended from $v=1.23$ to $v=3.0$.

IV. MEASUREMENTS AND PRECISION

A. General Remarks

The beam energy losses were determined by the standard method of measuring the beam energies by electrostatic deflection with attenuation sample "in" and "out," Fig. 2. For the stopping power ratios it was sufficient to take the ratios of the respective deflecting voltage shifts necessary to return the beam to the analyzer exit slit. In each case, these voltage shifts were produced at the same analyzer plate, hence, no correction for change in the analyzer constant caused by a change in symmetry of the two plate voltages had to be applied.[6] The nonrelativistic behavior of a cylindrical electrostatic analyzer may be described in a convenient approximation[25] by giving a constant "k" such that the kinetic energy in eV of an ion of charge $z|e|$ traversing it on a central orbit concentric with the plates is $kz|e|V$ in a region at zero potential. V is the potential difference between the deflecting plates. Two such analyzers were used during the experiments; one with $k=45.7$ and one with $k=20.0$. This constant was used only to locate each ratio measurement on the energy, and hence, the velocity scale. As reference energy the mean between the sample in and sample out energies was taken. A knowledge of k was not necessary to obtain the ratio desired.

No energy loss—even in the thickest foils used—exceeded 20% of the respective mean energy, and any further corrections to this value as discussed by Porat and Ramavataram[26] were negligible.

The beam was supplied by the Cockcroft-Walton circuit of the University of Chicago, the mean high voltage of which was monitored to within 0.01% and held constant to approximately this limit.[27]

The gas fed to the radio-frequency ion source was helium with about 0.8% deuterium and hydrogen added. The resulting beam contained these components in about equal proportions, as was revealed when they were sorted out by magnetic deflection. For some of the

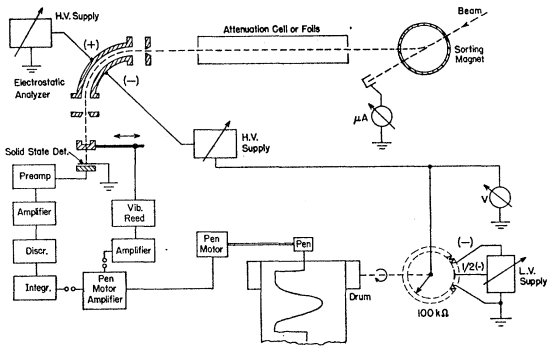

FIG. 2. Schematic diagram of the experimental equipment.

data, particularly in the lower energy range, the desired ratio was obtained by measuring the energy decrement produced in the He^+ beam which had been accelerated by the kevatron at voltage $\mathcal{U}$, then reducing the voltage to $\frac{1}{2}\mathcal{U}$ or $\frac{1}{4}\mathcal{U}$, and measuring the decrement produced in the D^+ or H^+ beam, respectively.

If no absorber was in the beam, the D^+ component and any H_2^+ present would not be separated by the magnetic and subsequent electrostatic deviations. Experiments with no deuterium in the ion source, however, disclosed a H_2^+/H^+ ratio of 0.06, which indicates a H_2^+/D^+ ratio of 0.03 when the gas added to the helium contained equal amounts of hydrogen and deuterium. Actually the presence of a small H_2^+ component does not vitiate the experiment, since it is entirely dissociated in passing through the absorber and then cannot follow the electrostatic deviation.

Although the maximum accelerator voltage was 460 kV, the measurements could be extended to include helium ions with kinetic energies of 920 keV by using the small He^{++} constituent put out by the ion source.[28] In this case, it is not necessary to lower the accelerator voltage in measuring the deuterium ions since D^+ and He^{++}, which have been accelerated together, have the same velocity.

The stopping power of isotopic projectiles such as D and H, compared at equal velocities, is the same if nuclear and atomic stopping effects can be disregarded. At high velocities this is the case, and Hall and Warshaw[29] and Phillips[16] have shown, and the present measurements confirm, that also at lower velocities where charge changing collisions become important, the stopping powers for D and H beams are equal. One can conclude that the same must be true for the effective charges. The difficulty in separating out the He^{++} from the much stronger D^+ was avoided by making use of the following fact. Even with the foil absorber out of the beam, or with "gas out" of the absorption cell, the pressure in these compartments was not sufficiently low to prevent some electron capture by the He^{++}. Thus, by

Particles in Matter of the Committee on Nuclear Science of the National Academy—National Research Council, 1961 (unpublished).

[22] P. K. Weyl, Phys. Rev. **91**, 289 (1953).

[23] H. K. Reynolds, D. N. F. Dunbar, W. A. Wenzel, and W. Whaling, Phys. Rev. **92**, 742 (1953).

[24] J. A. Phillips, Phys. Rev. **90**, 532 (1953).

[25] S. K. Allison, S. P. Frankel, T. A. Hall, J. H. Montague, and S. D. Warshaw, Rev. Sci. Instr. **20**, 735 (1949), Eqs. (39) and (42).

[26] D. I. Porat and K. Ramavataram, Proc. Phys. Soc. (London) **A252**, 394 (1959).

[27] M. N. Huberman (Ref. 6), Fig. 2.

[28] S. K. Allison and E. Norbeck, Jr., Rev. Sci. Instr. **27**, 285 (1956).

[29] T. A. Hall and S. D. Warshaw, Phys. Rev. **75**, 891 (1949).

doubling the deflecting voltage on the electrostatic analyzer, a detectable beam of He^+ could always be obtained, and its energy decrement noted. In such cases the desired ratio was obtained in a few moments, since the kevatron beam did not need to be refocused at a lower energy for the comparison with deuterium. This high-energy helium beam will hereafter be referred to as the $He^{++} \rightarrow He^+$ beam.

B. Apparatus and Performance

In Fig. 2 the experimental setup is shown schematically. After magnetic deflection the beam passes the gas attenuation cell or foil and then traverses the electrostatic analyzer.

The outgoing beam is detected with a vibrating reed electrometer (sensitivity variable between 10^{-12} and 10^{-6} A) or, for detection of the weak $He^{++} \rightarrow He^+$ beam, by particle counting with a solid-state detector and counting-rate integrator.

An automatic recording of the energy spectra was obtained in the following simple way: The precision regulated high-voltage supplies, connected to the outer and inner plates of the electrostatic analyzer, were adjusted to a voltage somewhat lower than the beam deflection voltage. The negative supply was insulated from ground and connected to a potentiometer across which a convenient adjustable smaller voltage was applied. This potentiometer was driven by the rotating drum of a Brown Recorder, the pen of which was deflected by the beam current, as shown. In this way a sort of slow sweep oscilloscopic recording of the energy spectra was obtained. The potentiometer had no stop, hence, the recording repeated itself in cycles.

The linearity of the device was tested by feeding part of the potentiometer output back into the electrometer input. The automatic recorder then traced straight lines; the deviation from linearity was of the order of 0.5% of the mean deflection.

Figure 3 shows spectra recorded with a 120-keV

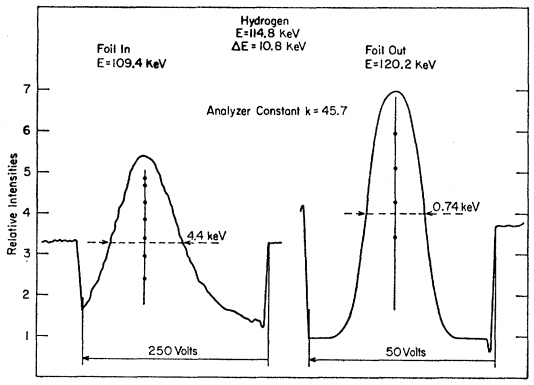

FIG. 3. "Foil-out" and "foil-in" curves registered for a 115-keV proton beam penetrating cadmium foils. The resolving power of the analyzer would produce a curve of about 0.5% half-width from a monoenergetic beam.

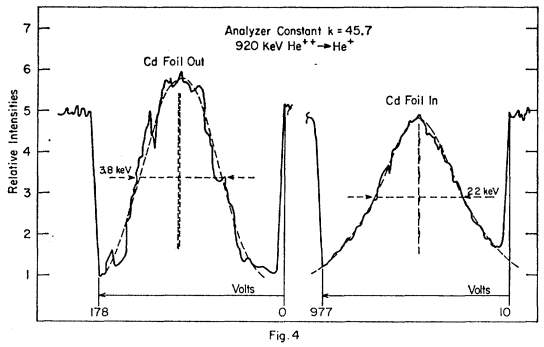

FIG. 4. "Foil-out" and "foil-in" intensity versus energy curves registered for 920-keV $He^{++} \rightarrow He^+$ beams penetrating Cd foils. The sensitivity of the sweep for a given change in energy has been greatly reduced in the "foil-in" curve to allow for the broadening due to energy straggling.

hydrogen beam, with "foil in" and "foil out," respectively. The change in the deflecting voltage corresponding to a given displacement along the abscissa is indicated by the energy scales at the bottom of the figure. The energy spectra are single peaked and symmetric and permit an evaluation of the energy loss in the foil with less than $\pm 0.5\%$ error. The half-width of the "foil-out" spectrum is about 0.6% of the peak energy; the energy straggling produces approximately a 4% half-width for the "foil-in" spectrum.

The sharp edges marked by arrows give reference points for the minimum ($\sim$zero) and maximum deflector voltages during the horizontal sweep. They are produced by letting the sliding point of the potentiometer pass a charged contact (Fig. 2). The total sweep voltages were measured with a calibrated meter and adjusted to have the breadth of the spectra sufficient for precise evaluation. A possible shift of the spectra caused by a delay in the recorder response was shown to be negligible by taking several spectra with sweep voltages varying as much as two to one. The corresponding peak voltages were equal within ± 0.3 V out of 4064.6 V applied across the analyzer.

The deflector voltage shifts due to the beam energy attenuations in the samples were of the order of 1500 V maximum, and usually the change was made by varying the voltage on the negative of the precision high-voltage supplies. The peak voltages of the recordings, obtained from the total sweep voltages by linear interpolation, had to be added to the negative voltage read on the meter of the high-voltage supply.

The two high-voltage supplies for the analyzer plates were checked against each other by opposition and found to coincide within 2 V throughout their range up to 10 kV. Voltage variations up to 2000 V were checked and found equal within 0.5%.

Figure 4 shows spectra obtained with the 920-keV $He^{++} \rightarrow He^+$ beam. The He^+ particles are registered with the solid-state detector—counting-rate meter combination. Although there are fluctuations in the

counting rate, it is clear that the spectra are sufficiently symmetric to permit localization of the peaks on the voltage scale within ± 0.5 V in the "foil-out" case and ± 4 V in the "foil-in" case. With 1.435-kV total voltage shift due to attenuation in the foil, the precision of its determination from the graphs is $\pm 0.3\%$.

With an appropriate discriminator setting, the solid-state detector had constant sensitivity throughout the energy range determined by the width of the "sample-in" curves, together with a high signal-to-noise ratio (>1000), even down to 160-keV He^+. Too high a discriminator setting resulted in considerable deformation and asymmetry of the resulting spectra.

In some cases the $He^{++} \rightarrow He^+$ beam intensity was sufficient to be detected with the electrometer ($\sim 4\times 10^{-12}$A). Within the above error limits, direct current reading yielded the same spectra as particle counting.

C. Measurements in Cd Foils

The preparation of the unbacked Cd foils used has been described elsewhere.[30]

Measurements with the foil in the beam path were always enclosed between "foil-out" runs and the corresponding mean value of the energy taken. For the same foil the He runs were followed immediately by the corresponding D runs, or vice versa. At energies higher than 100 keV/amu the measurements with hydrogen were included, and the He runs made between D and H runs. As mentioned in the introductory section of this paper, the energy attenuations of D and H beams of equal velocity coincided within a mean accuracy of 2%.

Different foils, covering a threefold variation in thickness were used for each determination of the stopping power ratio $Z^2\gamma^2$. The thinnest foil used produced an energy loss of 6.7 keV out of 400 keV for D, or only 1.7% of the beam particle energy.

In several cases the stopping power ratio was determined using for He the He^+ beam, as well as the $He^{++} \rightarrow He^+$ beam, which was weaker by a factor of 10^4. The resulting energy attenuations coincided within the experimental errors.

Table I gives a summary of all the measurements made on solid cadmium. We have used the notation $Z^2\gamma^2$ [Eqs. (8) and (5)] to represent the stopping power ratio ϵ_{He}/ϵ_H, conforming to the notation of Northcliffe[3] and Roll and Steigert,[20] in spite of the fact that here γ^2 cannot represent the square of the effective charge per atomic number of the heavy ion, since it is certain that the hydrogen beam with which it is being compared contains H^0. The errors shown in the last column are obtained directly from the statistics of the respective measurements, made with different foils and sometimes different equipment or methods. If there were more than $n=5$ measurements at the same beam velocity, the assigned error is the error of the mean value, or $n^{-1/2}$ times the mean absolute error. For $n<5$, this factor was not taken into account. In no case is the error greater than 2%, and in the mean it is of the order of 1.3%.

TABLE I. Solid cadmium. Measured stopping power ratios at various beam velocities v.

v (units of $e^2/\hbar$)	E_{He} (MeV)	$Z_{He}^2\gamma_s^2=[(\epsilon_{He})/(\epsilon_{H\text{ or }D})]_v$ $Z^2\gamma_s^2$	$\Delta(Z^2\gamma_s^2)$
1.22	0.148	2.21	0.03
1.38	0.190	2.35	0.02
1.51	0.228	2.44	0.03
1.65	0.273	2.62	0.02
1.80	0.324	2.73	0.04
1.95	0.380	2.88	0.02
2.14	0.460	2.91	0.05
2.37	0.560	3.10	0.03
2.60	0.675	3.20	0.04
2.79	0.780	3.42	0.04
3.00	0.900	3.50	0.04

The limits of precision and possible sources of systematic errors due to the measuring procedure have already been mentioned. Their influence must be considered small compared with the above error limits, and the main source of errors attributed to the foils themselves.

The uniformity of the foils was tested by measuring the stopping of the beam in different portions, resulting in deviations of less than 2%. Nevertheless, the foil positions were carefully reproduced in subsequent runs with He, D, or H.

The main source of error probably was due to surface layers, which in some cases would have affected absolute stopping-power measurements by up to 10%, but were almost cancelled out in the stopping power ratios, as shown by remeasuring with freshly prepared foils.

D. Measurements with Cd Vapor

The vapor pressure of Cd at its melting point (~ 320°C) is 100 μ Hg; at 350°C it reaches 250 μ Hg. It was, therefore, sufficient to use an attenuation cell provided with moderate heating, as seen in Fig. 5. The

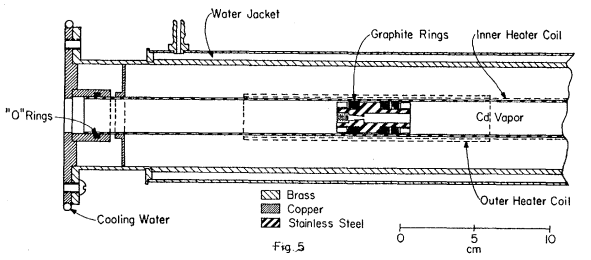

FIG. 5. The Cd-vapor absorption tube. The rate of escape of Cd through the apertures was negligible. The graphite rings were a satisfactory solution to difficulties with inserts sticking after heating. The inserts had sufficient friction to hold them in place; they could be positioned by detachable rods.

[30] W. Meckbach, Rev. Sci. Instr. **34**, 188 (1963).

entrance and exit ends of the cell are the same; only one is shown.

The central stainless steel tube is heated by a winding of Nichrome ribbon. The attenuation length (~50 cm) is between two pistons with tapered diaphragms (diam ~1 mm) to let the beam through. Its vacuum-tight and water-cooled telescoping supports on both ends allow for thermal elongation without producing misalignment with respect to the beam. An outer water jacket provides a constant surrounding temperature. For alignment the equipment is mounted on two adjustable frames (not shown), one of which is situated in the plane of the diaphragm through which the beam enters.

The two pistons had to be provided with graphite piston rings which permitted a smooth gliding motion combined with tightness, even after having applied heat. Additional heating was applied to the sections at the locations of the pistons. This prevents Cd vapor from condensing and obstructing the entrance or exit openings.

The Cd sample was put in the central section of the cell where the temperature was lowest and controlled by a Chromel-Alumel thermocouple connected to a potentiometer which permitted observation of temperature variations of less than 0.01°C. The ac heater current was regulated by a magnetic stabilizer. Slight fluctuations of the oven temperature could be held by hand within less than 0.05°C limits. This was compatible with 0.5% error in the Cd vapor pressure used for the measurements, and hence, the measured energy attenuations. Vapor pressure measurements were unnecessary since only stopping power ratios were required.

In order to minimize the time delay between "vapor-in" (oven-hot) and "vapor-out" runs to about 3 min, a blast of cold air could be applied to the central part of the tube.

Before putting in Cd, the cell was carefully outgassed at 400°C. Shifts of the simultaneously recorded energy spectra were observed only during the first 8 min of the total of 3 h outgassing time. After inserting the Cd and raising the temperature, a second outgassing was indicated by a strong beam energy attenuation which later, on maintaining a constant temperature, stabilized itself at a lower value. To be sure that this attenuation was due to Cd vapor alone, the energy shift was determined at two different temperatures such that the Cd-vapor pressure changed by a ratio of 2.46:1; the result was a corresponding ratio of energy attenuation of 2.49:1, which agreed with the change of pressure to within 1.2%.

A constancy test of the energy spectra, taken at 343°C with 300-keV incident He^+ ions is seen in Fig. 6. The accelerator had been running for 3 h at this voltage and the cell heated for about 50 min. Spectrum 2 was taken 70 min after spectrum 1. A shift of only 0.6 V out of 6161 V across the electrostatic analyzer is indicated.

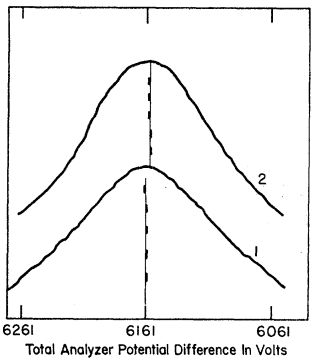

FIG. 6. A constancy test of the energy spectra taken at 197 μ Hg of Cd vapor with 300-keV He^+ ions. Spectrum 2 was taken 70 min later than No. 1, showing that the temperature control was adequate.

For convenience all the measurements on Cd vapor were made with the $He^{++} \rightarrow He^+$ and the D beam. First, with the cell at room temperature a deuterium spectrum was taken at the desired energy. Then the corresponding He spectrum was taken, for which it was only necessary to double the voltage on each analyzer plate. The temperature in the absorption cell was then raised to 334.0°C or approximately 150 μ Hg Cd vapor pressure. The shift of the He spectrum was continually observed until its position on the analyzer voltage scale became stabilized. After having taken several He spectra at this vapor pressure, the analyzer plate voltages were again lowered to take the "vapor-in" spectra with the deuterium beam. Finally, the temperature in the oven was quickly lowered as described and the "vapor-out" spectra were again taken, first with D, then with He. According to this schedule, the time elapsed between the "vapor-in" and final "vapor-out" spectra was:

for D of the order of 5 min,

for He of the order of 20 min.

The sequence of measurements was taken purposely in this way because greater care had to be taken with the D beam, which was less attenuated.

Table II shows the results of the measurements on Cd vapor. The errors assigned to the $Z^2\gamma^2$ values are

TABLE II. Gaseous cadmium. Measured stopping power ratios at various beam velocities v.

v (units of $e^2/\hbar$)	$Z_{He}{}^2\gamma_0{}^2=[(\epsilon_{He})/(\epsilon_D)]_v$ E_{He} (MeV)	$Z^2\gamma_0{}^2$	$\Delta(Z^2\gamma_0{}^2)$
1.25	0.156	2.03	0.03
1.39	0.195	2.22	0.03
1.53	0.235	2.29	0.03
1.68	0.282	2.38	0.03
1.82	0.331	2.54	0.02
1.99	0.394	2.58	0.03
2.18	0.474	2.74	0.03
2.44	0.594	3.00	0.05
2.62	0.689	3.28	0.04
2.82	0.794	3.49	0.05
3.02	0.914	3.74	0.05

based on the statistics of the repeated spectra taken in Cd vapor. At certain energies measurements have also been repeated and mean values taken.

As in the measurements with foils, the error limits were larger than expected. They probably have to be assigned to a lack of vapor-pressure equilibrium in the attenuation cell, which could be still improved by making sure that the Cd sample at any time is located at the coolest section of the oven, in which case no condensation of Cd can occur in any other place within the tube.

V. DISCUSSION OF MEASUREMENTS

By extrapolation of the data of Porat and Ramavataram[26] on ϵ for He projectiles in Ag, we estimate that the atomic stopping power of cadmium for He is about 72×10^{-15} eV cm^2/atom at 148 keV.

According to Bohr,[31] the contribution to the atomic stopping power from momentum and energy transfer to target nuclei is

$$\epsilon_n=\frac{4\pi\hbar^2Z^2Z_t^2}{M_tv^2}\ln\left[\frac{\mu v^2}{mZ_tZ(Z^{2/3}+Z_t^{2})^{1/2}}\right]\frac{\text{ergs cm}^2}{\text{atom}}, \quad (13)$$

where Z_t and M_t are the atomic number and mass of the target nuclei, μ is the reduced mass of projectile and target, m is the electronic mass, and v is the projectile velocity in units of $e^2/\hbar$. The largest value of this quantity which could be encountered in our experiments is at the lowest energy; at 148 keV we obtain $\epsilon_n=9.7\times10^{-16}$ eV cm^2/atom. However, in the derivation of Eq. (13), the energy losses for encounters which produced angular deviations less than

$$\theta=2ZZ_t(Z^{2/3}+Z_t^{2/3})^{1/2}m/\mu v^2\sim0.06 \text{ rad}$$

were neglected. In our case, the angular spread of the beam was limited to 0.002 rad in the horizontal plane and 0.013 in the vertical. Hence, losses due to nuclear encounters do not contribute appreciably to our results.

The atomic stopping power ratio of He to D or H in gaseous and solid cadmium is graphically illustrated in Fig. 7. The ordinates are the values $Z^2_{He}\gamma^2$ from Eqs. (8)

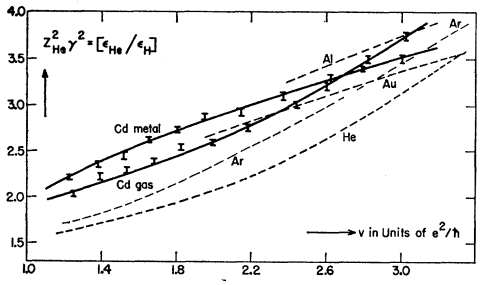

FIG. 7. Stopping-power ratios measured in these experiments (heavy lines) compared to data in other substances obtained by combining the results of various experimenters.

and (5), and Tables I and II. An outstanding feature of the results is that at these beam velocities, well within the electron capture and loss region, the stopping-power ratio is, to within 8%, the same for Cd vapor and solid Cd. To interpret this fact in terms of a change of effective charge of the beam, we would need more information than is now available concerning the charge states and partial atomic and ionic stopping powers in cadmium. The research of Allison *et al.*[5] and of Huberman[6] have made this information available for hydrogen beams in hydrogen gas, however, and give some idea of the sensitivity of ϵ_H as a measure of i or $\langle i^2\rangle_{av}$. If we neglect the insignificant contribution from negative hydrogen, the conventional stopping power ϵ for a hydrogen beam in H_2 gas may be written

$$\epsilon=F_{0\infty}\epsilon_0+F_{1\infty}\epsilon_1+\sigma_c(W_{01}+W_{10}), \quad (14)$$

where ϵ_0 is the partial stopping power for atomic hydrogen projectiles without contributions from charge changing collisions, in eV cm^2/atom; ϵ_1 is the analogous partial stopping power for protons; $\sigma_c=\sigma_{01}\sigma_{10}/(\sigma_{01}+\sigma_{10})$, where σ_{01} is the loss and σ_{10} the capture cross section in cm^2/atom; $(W_{01}+W_{10})$ is the energy loss in eV incurred in the completion of a charge-changing cycle.

Since $F_{1\infty}=\sigma_{01}/(\sigma_{01}+\sigma_{10})$ and $F_{0\infty}+F_{1\infty}=1$, we may write

$$\epsilon=\epsilon_0+F_{1\infty}[\epsilon_1+\sigma_{10}(W_{01}+W_{10})-\epsilon_0] \quad (15)$$

and obtain

$$\frac{\partial\epsilon}{\epsilon}=\frac{\epsilon_1+\sigma_{10}(W_{01}+W_{01})-\epsilon_0}{\epsilon}\partial F_{1\infty}=\frac{\epsilon-\epsilon_0}{\epsilon}\frac{\partial F_{1\infty}}{F_{1\infty}}. \quad (16)$$

Table III shows the percentage change in ϵ caused by 1% change in the fraction of protons in the beam and in the last column it is seen that above 60 keV such a change leads approximately to a 0.7% change in ϵ. This is the only guide we have to conditions of the H beam in cadmium absorbers.

In the region $v=2.4$ to 3.0, the value of $F_{1\infty}$ for H in gases such as H_2 and N_2 increases from 0.90 to 0.98,[32]

TABLE III. Sensitivity of stopping power of H_2 gas for hydrogen to a change in the fraction of protons in the beam [Eq. (16)].

Kinetic energy (keV)	v	ϵ's$\times10^{15}$ eV$\times$cm^2/atom $F_{1\infty}$	ϵ_1	ϵ_0	ϵ	% change in ϵ due to 1% change in $F_{1\infty}$
20	0.89	0.185	5.0	3.3	5.0	0.34
40	1.26	0.380	6.2	3.0	6.3	0.53
60	1.55	0.553	6.3	2.4	6.6	0.64
80	1.79	0.724	6.2	2.0	6.2	0.68
100	2.00	0.817	5.7	1.9	5.8	0.67
125	2.24	0.877	4.9	1.8	5.3	0.66
150	2.45	0.937	4.0	1.6	4.6	0.65

[31] N. Bohr, Kgl. Danske Videnskab. Selskab, Mat. Fys. Medd. **18**, No. 8 (1942).

[32] P. M. Stier and C. F. Barnett, Phys. Rev. **103**, 896 (1956).

and in the beam emerging from a fresh aluminum surface[16] it varies from 0.96 to 0.99. It seems unlikely that a change $\partial F_{1\infty}$ in the effective charge of more than 2% from gas to solid could be expected for a D or H beam of these velocities. In this upper velocity region of Fig. 7, it is seen that

$$1<[\epsilon_{He}/\epsilon_H]_{gas}/[\epsilon_{He}/\epsilon_H]_{solid}<1.06. \quad (17)$$

Since by Table III, a 2% change in $F_{i\infty}$ means a similar change in ϵ_H, we can conclude that ϵ_{He} does not vary by more than 8% from Cd vapor to Cd gas in this velocity region. If we anticipate in Cd vapor about the same charge composition as in air, He^0 is less than 2% throughout this velocity range, in which He^{++} rises from $F_{2\infty}=0.43$ to 0.75 and $F_{1\infty}+F_{2\infty}=1$. Due to the presence of the higher charged state (He^{++}) the variation of ϵ_{He} with effective charge is expected to be more rapid than that for H shown in Table III. Thus, we may state that the effective charge of the helium beam in the kinetic energy range 575–920 keV changes by less than 8% from rarefied Cd vapor to Cd metal. Within this interval, the sign of the change seems to reverse, the effective charge being actually greater in the rarefied vapor above 730-keV kinetic energy. These are small changes compared to the 79 to 95% increase in $\bar{i}$ found by Lassen for 6.6×10^8 cm/sec fission fragments in solids compared to gases, or the 20% increase in γ^2 cited by Roll and Steigert for fluorine ions.

In the lower velocity range from 1.2 v_0 to 2.6 v_0, we cannot safely set bounds to the possible change of ϵ_H between the gaseous and solid phases, and our deductions are less quantitative. The fact that the ratio in the solid exceeds that in the gas by less than 8% indicates no profound change in the electron retention of either the H or the He beam from one environment to the other. For if the charge change were large compared to the upper limits of 1 and 2 for H and He, respectively, it is improbable that the ratio should be affected as little as is observed experimentally. It is unsafe to give a numerical value to the possible small change which cannot be excluded, until further experiments are performed, such as an accurate comparison of the atomic stopping power of Cd solid and Cd vapor for a H or for a He beam.

Let τ_r be the time required for dissipation of the excitation energy if an ion captures an electron into an excited orbit, and τ_c be the interval of time between successive capturing collisions. Bohr and Lindhard[10] have ascribed the enhancement of effective charge of fission fragments in a solid to the fact that $\tau_r/\tau_c\gg1$ in the solid, and $\tau_r/\tau_c\leqslant1$ in the gas. We may inquire whether these inequalities are also true for the helium atoms in our case. To obtain an estimate of the radiation time, we use the classical theory of radiation damping,[33] which gives

$$\tau_r=3mc^3/4\pi^2e^2\nu^2,$$

where ν is the frequency of radiation in sec^{-1}. If the energy to be radiated away after a capture by He^+ is 20 eV, we obtain $\tau_r=3.7\times10^{-10}$ sec.

In Cd vapor at 160 μ Hg pressure at 6×10^8 cm/sec, the He projectile has an interval τ_c of 2.5×10^{-9} sec between collisions with Cd atoms if we take the charge-changing cycle cross section σ_c as 15×10^{-17} cm^2. In solid cadmium τ_c is about 2.4×10^{-16} sec. Thus, we have

$$\begin{aligned}&\text{Cd vapor,}\quad (\tau_r/\tau_c)_{He}\sim0.15;\\ &\text{Cd metal,}\quad (\tau_r/\tau_c)_{He}\sim1.5\times10^6;\end{aligned} \quad (18)$$

so that the change of environment as regards ratio of radiation to collision time is indeed severe, and the conditions for Bohr and Lindhard's explanation exist. If objections are raised to this type of explanation, for instance, that the radiation times quoted are far too small, due to initial capture of electrons in orbits of high angular momentum, or to metastable states, the explanation of the fission fragment behavior is also invalidated.

In summary, we can state that the changes in stopping power from gas to solid appear to be considerably less than those found by Lassen and by Roll and Steigert for heavier ions, although the change in the radiation-time versus collision-time ratio is as great as in the cases studied by them.

A theory of Neufeld[34] describes a density effect for He ions in condensed argon and argon gas in terms of the electrostatic field due to polarization of the medium traversed by a charged particle. This field is proportional to the density of the medium and produces field emission of any excited electron from He^+ in the condensed matter only, resulting in an effective charge squared about 12% higher than in argon gas. A direct comparison of the present data with this theory, applied to the case of Cd, is not feasible, because although the change to be expected in $\sum i^2F_{i\infty}$ is calculated, the relation between this measure of effective charge and stopping power will remain unclear for He in this velocity region, until the partial stopping powers for He^0, He^+, and He^{++} are known.

Empirically, data on ϵ_{He}/ϵ_H ratios, which are easier to measure than absolute stopping powers, are useful in converting absolute measurements on protons to absolute He values, and Whaling[35] has compiled a set of such ratios averaged over a few target substances and possibly accurate to 20%. These are obtained by combining the results of different experimenters with different measuring systems. Some of the results of such combinations are shown in the dashed curves of Fig. 7. The curves for argon and helium target gases combine data taken by Burgy[21] and by Weyl[22] on He projectiles,

[33] A. H. Compton and S. K. Allison, *X Rays in Theory and Experiment* (D. Van Nostrand, Inc., New York, 1935), p. 270.

[34] J. Neufeld, Phys. Rev. **96**, 1470 (1954).

[35] W. Whaling, in *Handbuch der Physik*, edited by S. Flügge (Springer-Verlag, Berlin, 1958), Vol. 54, p. 193.

and by Reynolds *et al.*,[23] Weyl and Phillips[24] on H projectiles. The curves for Al and Au combine data taken by Gobeli[36] on He and the data of many experimenters with hydrogen beams as collected by Whaling.[35]

In the high-energy region above 1 MeV per amu, Roll and Steigert, giving fluorine projectiles as a typical example show that $\epsilon_{M,F}/\epsilon_{M,H}$ ratios fall into two groups, one having a common and larger numerical value characteristic of solid targets as a class, and a group, characteristic of gases, having smaller numerical values. Figure 7 indicates that, unfortunately for the usefulness of $\epsilon_{He}/\epsilon_{H}$ ratios in this lower energy region, such a grouping into values typical of solids and gases probably does not occur, but that the difference between solids and gases is comparable to the difference between different gases (such as He and Ar) and different metals.

[36] G. W. Gobeli, Phys. Rev. **103**, 275 (1956).

ACKNOWLEDGMENT

Our thanks are due to John Erwood for extensive help in circuit construction and maintenance of the Cockcroft-Walton accelerator.

PHYSICAL REVIEW VOLUME 132, NUMBER 1 1 OCTOBER 1963

Dissociation Energy of $He_2^+(^2\Sigma_u^+)$†

P. N. REAGAN
Department of Physics, The University of Texas, Austin, Texas

J. C. BROWNE
Computation Center and Department of Physics, The University of Texas, Austin, Texas

AND

F. A. MATSEN
Departments of Chemistry and Department of Physics, The University of Texas, Austin, Texas

(Received 17 May 1963)

The potential curve for $He_2^+(^2\Sigma_u^+)$ has been calculated using Slater-type orbitals as a basis for a 26-term atomic orbital-configuration wave function. The calculation establishes a rigorous lower bound, E_{exp}(atoms) $-E_{calc}$(molecule), of 2.24 eV for the dissociation energy of $He_2^+(^2\Sigma_u^+)$. This value together with the ionization energies of $He^*(2\,^3S)$ and $He_2^*(^3\Sigma_u^+)$ is used in an energy cycle to give a lower limit of 1.76 eV for the dissociation energy of $He_2^*(^3\Sigma_u^+)$.

INTRODUCTION

THE helium molecule ion He_2^+ was first detected by Tüxen[1] in the mass spectrometer. The results of subsequent mass spectrometric investigations[2–4] have established that its mechanism of formation is

$$\begin{aligned} &\text{(a)}\ \ He+e \rightarrow He^*+e, \\ &\text{(b)}\ \ He^*+He \rightarrow He_2^++e, \end{aligned} \tag{1}$$

where He* is some excited state (s) of the helium atom. A lower bound for the dissociation energy of He_2^+ may, therefore, be determined by the equation

$$D_0(He_2^+) \geq I(He) - A.P.(He_2^+), \tag{2}$$

where A.P.(He_2^+) is the appearance potential of He_2^+ in the mass spectrometer. The most recent investigation[4] finds

$$D_0 \geq 1.5 \pm 0.3 \text{eV}.$$

An estimate of the interaction energy of a helium ion and a helium atom can be obtained from the scattering cross sections of the ion into helium gas. Mason and Vanderslice[5] computed a value of $D_e = 2.16$ eV ($D_e \cong D_0 + 0.1$) by analyzing the scattering data of Cramer and Simons[6] in terms of a Morse potential. The process of obtaining a potential curve from scattering data involves several uncertainties so that this result cannot on its own merit be regarded as reliable.

A third estimate for the dissociation energy of He_2^+ can be found from the energy cycle,

$$\begin{aligned} D_0(He_2^+(^2\Sigma_u^+)) = D_0(He_2^*(^3\Sigma_u^+)) \\ + I(He^*(2\,^3S)) - I(He_2^*(^3\Sigma_u^+)). \end{aligned} \tag{3}$$

The last two terms of the right member of Eq. (3) are known with high accuracy. Using a value of $D_0(He_2^*(^3\Sigma_u^+)) = 2.6$ eV, obtained by means of a linear

† Supported by the Robert A. Welch Foundation, Houston, Texas, and the U. S. Air Force Office of Scientific Research, Contract AF-AFOSR-273-63.

[1] O. Tüxen, Z. Physik **103**, 463 (1936).
[2] F. L. Arnot and M. B. M'Ewen, Proc. Roy. Soc. (London) **A177**, 106 (1939).
[3] J. A. Hornbeck and J. P. Molnar, Phys. Rev. **84**, 621 (1951).
[4] F. J. Comes, Z. Naturforsch. **17a**, 1032 (1962).
[5] E. A. Mason and J. T. Vanderslice, J. Chem. Phys. **29**, 361 (1958).
[6] W. H. Cramer and J. H. Simons, J. Chem. Phys. **26**, 1272 (1957).